Renewable and Sustainable Energy Reviews 16 (2012) 4352–4364

Contents lists available at SciVerse ScienceDirect

Renewable and Sustainable Energy Reviews

journal homepage: www.elsevier.com/locate/rser

A synthesis of numerical methods for modeling wave energy converter-point absorbers

Ye Li*, Yi-Hsiang Yu

National Wind Technology Center, National Renewable Energy Laboratory (NREL), Golden, CO 80401, USA

ARTICLE INFO

Article history:
Received 14 September 2011
Accepted 8 November 2011
Available online 5 June 2012

Keywords:
Wave energy converter
Wave theory
Point absorber
Numerical modeling
Wave–body interaction
Computational fluid dynamics

ABSTRACT

During the past few decades, wave energy has received significant attention for harnessing ocean energy. Industry has proposed many technologies and, based on their working principle, these technologies generally can be categorized into oscillating water columns, point absorbers, overtopping systems, and bottom-hinged systems. In particular, many researchers have focused on modeling the point absorber, which is thought to be the most cost-efficient technology to extract wave energy. To model such devices, several modeling methods have been used such as analytical methods, boundary integral equation methods and Navier–Stokes equation methods. The first two are generally combined with the use of empirical solution to represent the viscous damping effect, while the last one is directly included in the solution. To assist the development of wave energy conversion (WEC) technologies, this paper extensively reviews the methods for modeling point absorbers.

Contents

1. Introduction

While development of modern wave energy converter dates back to 1799 [1], the technology did not receive worldwide attention until the 1970s when an oil crisis occurred and Stephen Salter published a notable paper about the technology in *Nature* in 1974 [2]. In the early 1980s, after a significant drop in oil prices, technical setbacks and a general lack of confidence, progress slowed in the development of wave energy devices as a commercial source of electrical power. In the late 1990s, awareness of the depletion of traditional energy resources and the environmental impacts of the large utilization of fossil fuels significantly increased, thereby facilitating the development of green energy resources. The development of the wave energy technology grew rapidly, particularly in oceanic countries such as Ireland, Denmark, Portugal, the United Kingdom, and the United States. Several pre-commercial devices

* Corresponding author. Tel.: +1 303 384 6988; fax: +1 303 384 6950.
E-mail address: ye.li@nrel.gov (Y. Li).

1364-0321/$ – see front matter © 2012 Published by Elsevier Ltd.
doi:10.1016/j.rser.2011.11.008

were deployed. For example, a United States company, Ocean Power Technology, deployed one of their 150 kW wave energy conversion (WEC) systems in Scotland in 2011 [3]. An Irish company, Wavebob, tested a one-quarter scale model in Galway Bay, Ireland, in 2006 [4]. In Denmark, the half scale 600 kW Wave Star energy system was deployed at Hanstholm in 2009 [5], and a quarter and a half size model Wave Dragon was tested at Nissum Bredning in 2003 [6]. Furthermore, international organizations, such as the International Energy Agency and the International Electrotechnical Commission, are heavily involved in the development of wave energy devices. In 2001, the International Energy Agency established an Ocean Energy System Implementation Agreement to facilitate the coordination of ocean energy studies between countries [7]. In 2007, the International Electrotechnical Commission established an Ocean Energy Technical Committee to develop ocean energy standards [8].

1.1. Device design

To date, there are more than one hundred prototypes of various WEC systems [7]. They can be sorted into a few types. According to their energy conversion principles, WEC systems include oscillat-

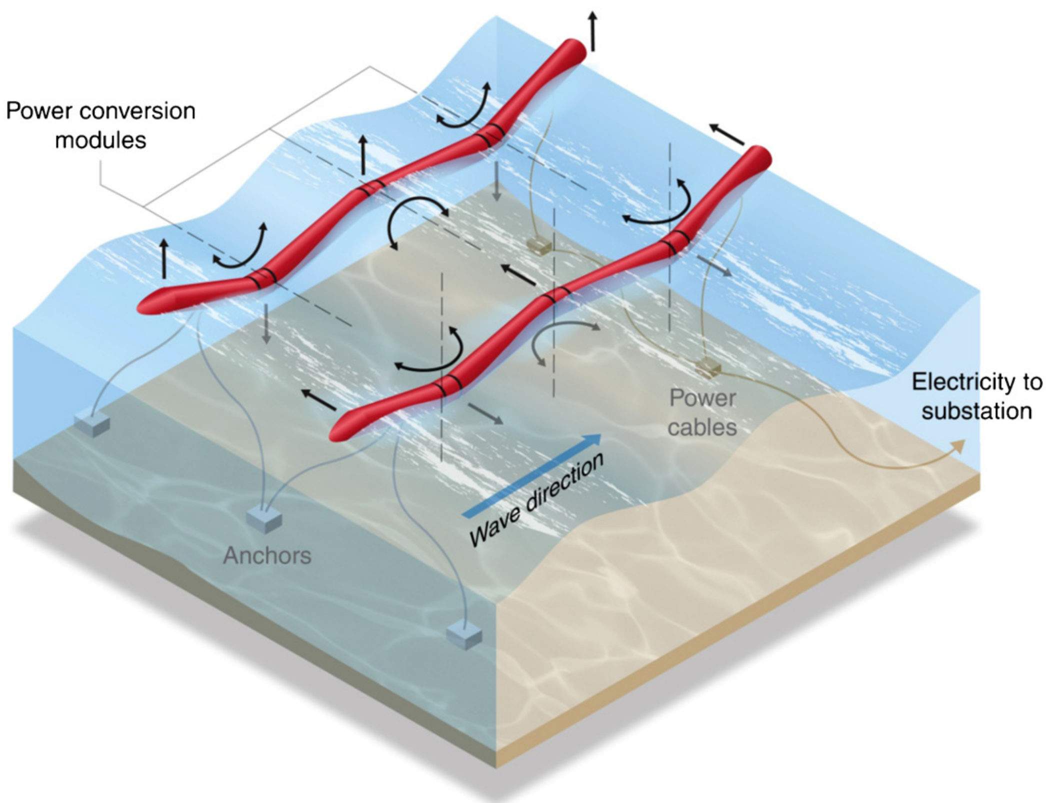

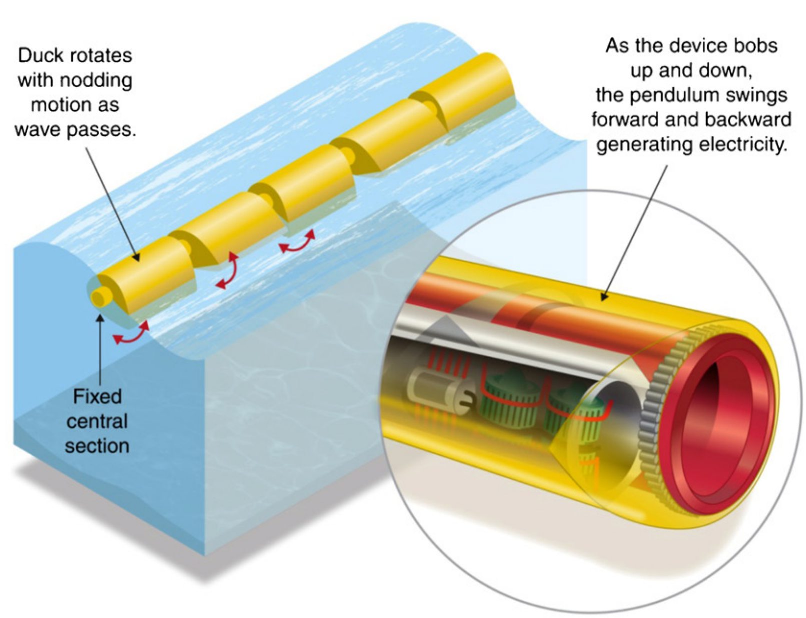

Fig. 1. An illustration of the floating-pitching devices: (top) multiple degree of freedom and (bottom) single degree of freedom. Illustration by Al Hicks, NREL.

ing water column, overtopping system, pitch device, membrane, and point absorber. Most of these can be both bottom-mounted and floating. A brief introduction on the working principle of different types of WEC system is given in this section, but the focus of this paper is on point absorbers.

The floating-pitching device, whether it is composed of a single body or a number of connecting bodies, has rotational freedom (Fig. 1). The device converts wave energy from its pitching motion. The principal axis for floating-pitching devices is either perpendicular (terminator) or parallel (attenuator) to the wave direction. Among various developments since the 1970s, Salter proposed one of the most significant inventions in 1974 [2], which became the well-known Salter's Duck (also referred to as the Edinburgh Duck). The Salter's Duck and PS Frog Mk 5 [9] are two examples of the terminator, and McCabe Wave Pump [10] and Pelamis [11] are the examples of the attenuator. A wave farm consisting of 750 kW Pelamis devices was tested in northern Portugal in 2008 and another farm was deployed in Orkney, Scotland, in 2010.

The bottom-hinged pitching system includes a paddle, or a flap, that is connected to a hinge deflector on the seabed; the top of the device is generally above the free surface (Fig. 2). It is sometimes called a wave surge converter, because it converts wave energy from the horizontal movement of the water particles. Unlike the floating-pitching device, one end of the bottom-hinged device is fixed. That is, it shares a similar working principle as the floating terminators, e.g., Salter's Duck in Fig. 1(bottom). Examples of the bottom-hinged pitching system include the swing mace, also proposed by Salter in the 1990s [12], and the Aquamarine Power Oyster [13], which was connected to the electrical grid and tested in Scotland in 2009 [14].

The oscillating water column includes a special chamber with a bidirectional turbine inside (Fig. 3). One end of the chamber has an inlet that allows the incident wave to enter and the other end contains the turbine. The device converts wave power by utilizing the wave elevation to compress or decompress the air in a chamber. The compressed air goes through a bi-directional turbine. The turbine is a Wells turbine conceived by Professor Alan Wells of Queen's University, in Belfast, in late 1970. A wide variety of oscillating water column devices include the LIMPET (shoreline system) [15], and Sakata (integrated into breakwater) [16].

The overtopping device includes a large structure that embraces the incident wave and an outlet with turbines inside the large structure (Fig. 4). The device converts wave power by utilizing the wave overtopping phenomenon to let the water fall through the outlet of the designed structure. When the water falls through the outlet, it passes one or more turbines similar to a traditional hydro dam; the potential energy is converted into electric power. The design involves both kinematic energy and potential energy in the conversion process. Examples include the Tapchan (shoreline system) [17], the Wave Dragon (offshore floating system) [18], and the Seawave Slot-Cone Generator (SSG), which was integrated into a breakwater [19].

The membrane device includes a membrane structure and a power conversion system that can be a turbine, piezoelectric, or other system (Fig. 5). The device converts wave power by utilizing the dynamic pressure change during wave propagation (e.g., Lilypad [20]).

A point absorber generally converts wave energy by utilizing the heave motion (Fig. 6). Note that there are few pitching point absorbers, such as PS Frog Mk5 [9], and they are considered as pitching devices in this paper. Typically, a point absorber is either a single-body that generates energy by reacting against a fixed seabed frame, or it is a multiple-body device that generates energy from the relative motion between the two bodies. There are many

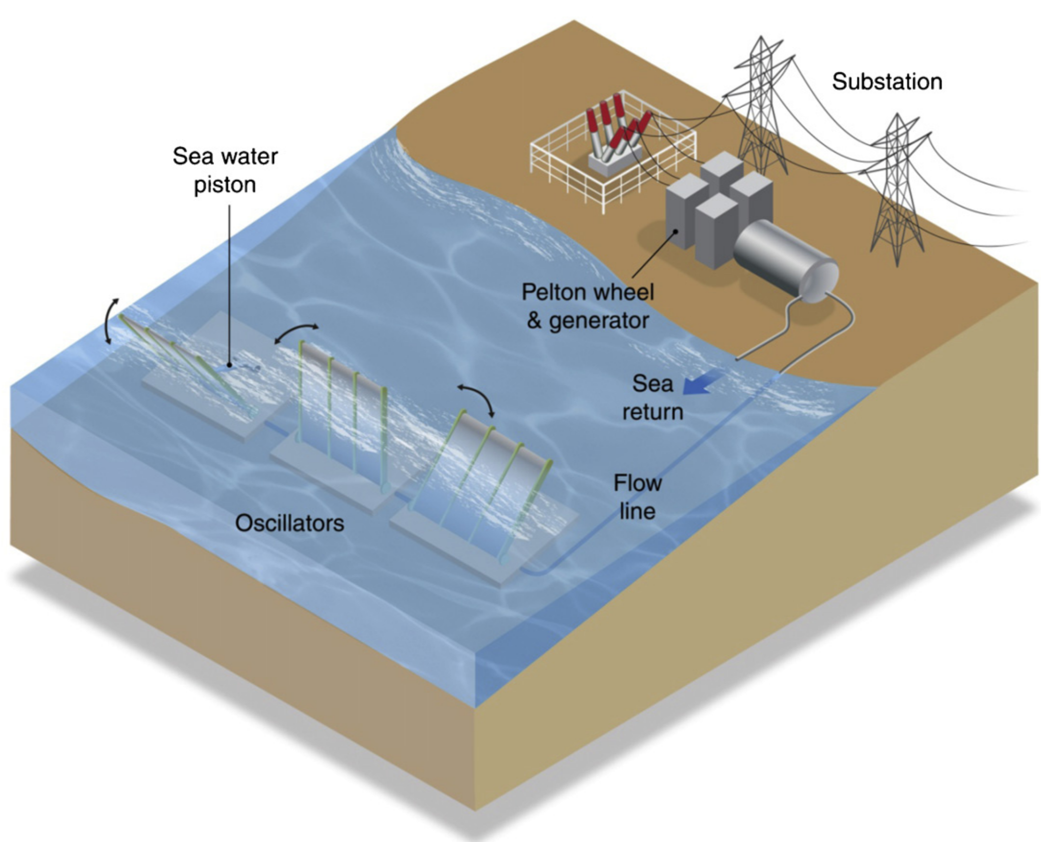

Fig. 2. An illustration of the bottom-hinged system. Illustration by Al Hicks, NREL.

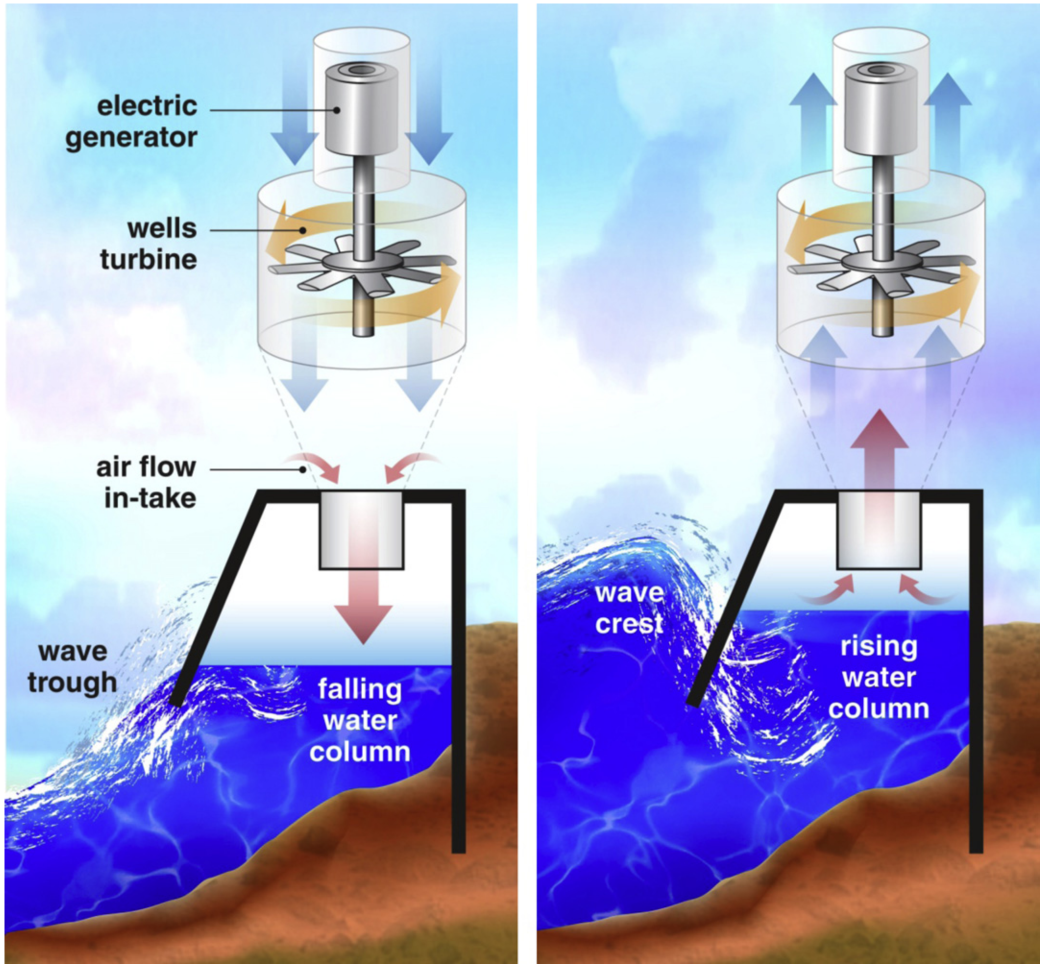

Fig. 3. An illustration of the oscillating water column. Illustration by Al Hicks, NREL.

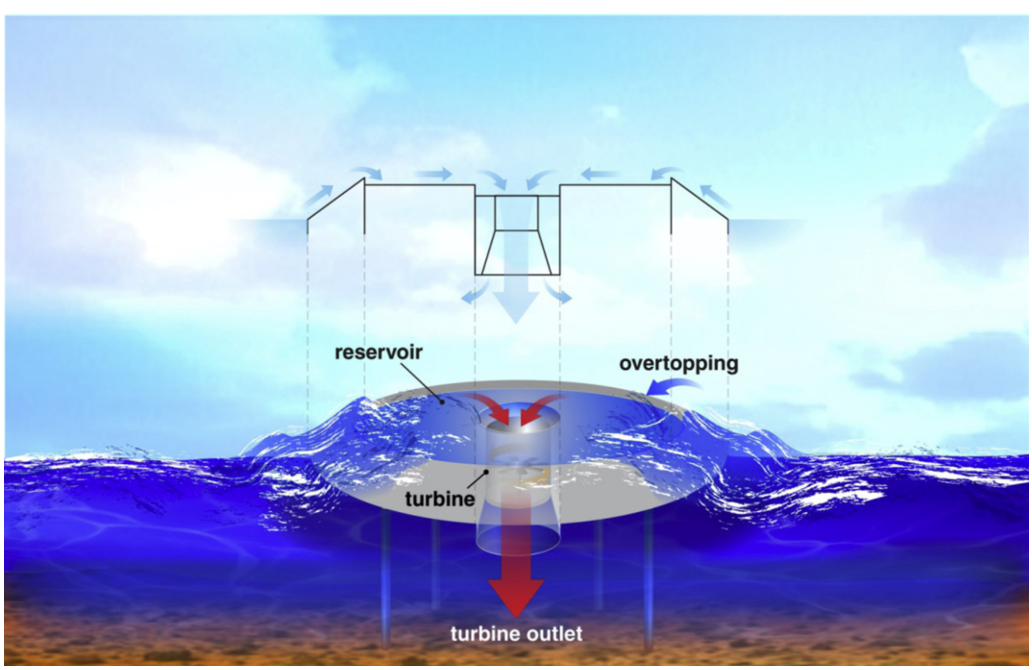

Fig. 4. An illustration of the overtopping device. Illustration by Al Hicks, NREL.

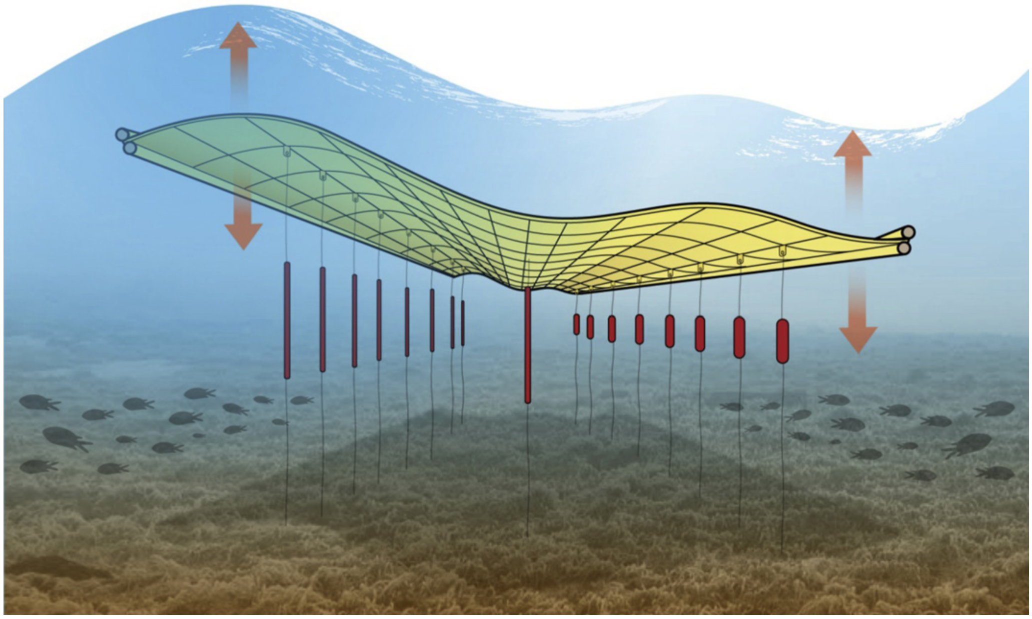

Fig. 5. An illustration of the membrane device. Illustration by Al Hicks, NREL.

popular devices such as the OPT PowerBuoy [16], Wavebob [21], and Inter Project Service buoy [22–24]. Since the point absorber is the focus of the paper, its principles are described in greater detail in Section 2.

1.2. Objective of this paper

Several literature reviews of WEC devices have been published providing information about various aspects of the technology. For example, Evans reviewed the analytical derivation of the absorber's motion [25]. Falcão provide a comprehensive overview of the history and status of the development of WEC systems [26]. Sarmento discussed the non-technical aspects of the technology during its commercialization path [27]. The U.S. Department of Energy (DOE) developed a database to document various technology characteristics [28]. Some concise reviews reporting interim progress were written by several researchers, such as Falnes [29], on theoretical limits [29], and Khan et al. [30], on interconnection issues. There also are introductory textbooks on this subject such as *Wave Energy Conversion* by Brooke [31], *Ocean Wave Energy* by Cruz [32], *Ocean Wave Energy Conversion* by McCormick [33], and *Ocean Waves and Oscillating Systems* by Falnes [34].

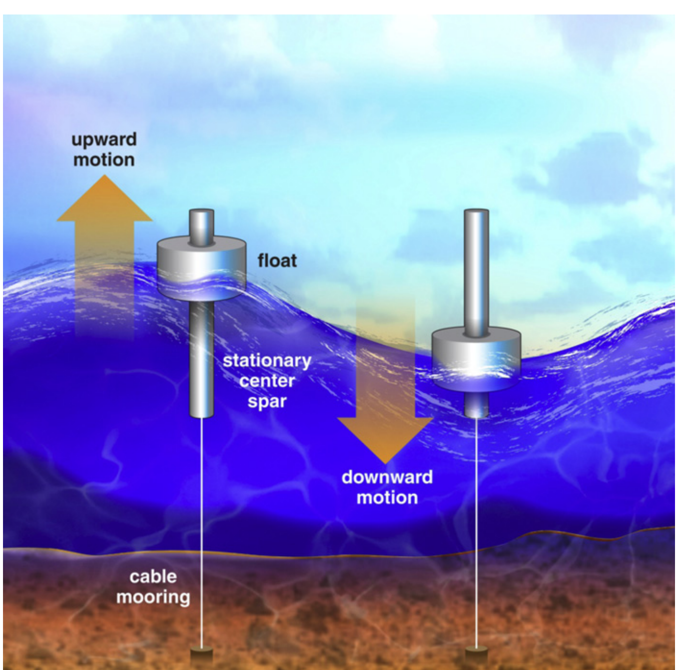

Fig. 6. An illustration of the point absorber. Illustration by Al Hicks, NREL.

However, to date, there has been no systematic review of modeling methods. The rapid development has not led the industry to a commercial stage yet. From a pre-commercial stage to a full-scale commercial stage, a good understanding of device performance and reliability is required. This requirement has not been met yet. In addition to these non-technology barriers, it is believed that a lack of understanding and quantification of the device behavior is one of the main reasons industry development has been delayed.

During the development of wave energy technology, many methods for modeling WECs were developed during the technology's evolution. To understand point absorber behavior, precise modeling tools are needed to simulate the dynamics of the device, along with a well-defined combination of modeling methods. Technology developers, engineers, and researchers need a guideline of which methods to employ for a specific purpose. To facilitate the development of the technology and help to model the device behavior more cost-effectively, we conducted a systematic review of various methods for modeling WECs. The reviews are summarized in this paper. Since there are a great number of device types, we will focus on the point absorber as an example. Additionally, we focus on the hydrodynamic modeling methods in this paper. Other modeling methods, such as electrical or control modeling, are not discussed, although they are important as well.

Specifically, this paper summarizes the numerical methods used for simulating point absorbers. After presenting the working principles of the point absorber, the paper details the existing modeling work that uses analytical approaches, empirical methods, and numerical methods. At the end, we compare the advantages and disadvantages of different hydrodynamic modeling methods.

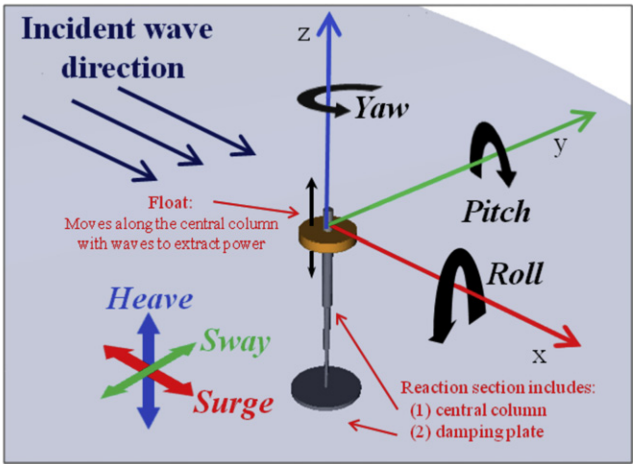

Fig. 7. The translation and rotation of the body (6 degrees of freedom).

2. Fundamentals of point absorbers

The simulation of point absorbers is a wave–body interaction topic. It requires knowledge of body dynamics and wave theory. Before we review the modeling methods for point absorbers, we review the fundamentals of body dynamics and wave theory.

2.1. Point absorber dynamics

The motion of a point absorber in six degrees of freedom is plotted in Fig. 7. The dynamics of the device can be expressed by the following equations,

$$\begin{aligned} m_b\mathbf{a}_t &= \mathbf{F}_{hd} + \mathbf{F}_{res} + \mathbf{F}_{PTO} + \mathbf{F}_{ext}, \\ \mathbf{I}_g\mathbf{a}_\Omega + \boldsymbol{\Omega} \times \mathbf{I}_g\boldsymbol{\Omega} &= \mathbf{M}_{hd} + \mathbf{M}_{res} + \mathbf{M}_{PTO} + \mathbf{M}_{ext}, \end{aligned} \tag{1}$$

where m_b is the mass of the body, $\mathbf{a}_t$ is the acceleration vector for the translation, $\boldsymbol{\Omega}$ and $\mathbf{a}_\Omega$ are the angular velocity and acceleration vectors, $\mathbf{I}_g$ is the moment of inertia tensor at the center of gravity, **F** and **M** are the resulting force and moment acting on the body. The subscripts '*hd*' and '*res*' represent the hydrodynamic excitation component, the restoring component, respectively. The subscripts '*PTO*' and '*ext*' represent the power take off (PTO) forces and the addition constraints, such as mooring line forces. Faltinsen [35] comprehensively reviewed the wave-induced motion and loads on offshore structures due to linear, nonlinear, and viscous effects. Note that the paper is mainly concerned with the prediction of the hydrodynamic components of the system. However, Evans [36] and Pizer [37] showed that additional constraints might further reduce the motion response of the device. The effect of the mooring constraint depends on its configuration and design. A discussion about the influence of the mooring system on the power generation performance of a two-body wave energy system was presented in Ref. [38].

Generally, single-body point absorber converts energy from the relative motion between the floating buoy and the seabed. Two-body system extracts energy from the relative motion between the two oscillating bodies, a float section, and a reaction section. The float is only allowed to move freely in one degree of freedom, with respect to the reaction section (generally in heave). When the PTO component was included, the additional PTO force F_{PTO} was considered. A mass–spring–damper system can be used to represent the PTO mechanism, and PTO force becomes

$$F_{PTO} = -C_{PTO}u_{rel} - kz_{rel}, \tag{2}$$

where z_{rel} and u_{rel} are the relative motion and velocity of the two bodies, k is the spring stiffness, C_{PTO} is the power absorption (damping) coefficient. The generated power from PTO is defined as

$$P_{PTO} = C_{PTO}u_{rel}^2, \tag{3}$$

which is proportional to the square of the relative translational velocity of the two sections. To optimize the power generation, different control strategies can be applied to the system. An introduction to latching phase-control was given in Ref. [39], and a review on the implementation of a spring in phase control, which is called reactive phase-control, was described in Ref. [26].

2.2. Free surface wave theory

The free surface waves are a representation of various forces, e.g., the wind or a ship, acting on and deforming the fluid surface against the action of gravity and surface tension. Naturally, waves occur in all sizes and forms. Depending on their magnitude, they act on the fluid along with other environmental conditions, such as bottom topography, temperature and fluid density. In general, waves can be described as linear or nonlinear, regular or irregular, unidirectional or omni-directional. The analytical solutions of free surface waves were derived based on the potential flow method, where the flow is assumed to be incompressible and irrotational. The velocity potential $\phi(\mathbf{X},t)$ therefore, is obtained by solving the Laplace equation

$$\nabla^2\phi = 0, \tag{4}$$

The exact solution of the above equation is very complex. We start the review at the linear wave theory, which is obtained using simplified assumptions. Linear wave theory, also referred to as small amplitude wave theory and airy wave theory [40,41], is the simplest solution (first-order approximation) for the flow field. For progressive gravity waves of period T, amplitude H, and water depth d, linear wave theory assumes H is much smaller than d and wavelength λ, and the boundary conditions are linearized. The kinematic free surface boundary condition (KFSBC) and the dynamic free surface boundary condition (DFSBC) are then reduced to

$$\begin{aligned} &\text{KFSBC}: \quad \frac{\partial\phi}{\partial z} - \frac{\partial\eta}{\partial t} = 0 \quad \text{at} \quad z = 0, \\ &\text{DFSBC}: \quad -\frac{\partial\phi}{\partial t} + g\eta = 0 \quad \text{at} \quad z = 0, \end{aligned} \tag{5}$$

where g is gravity. Both the linearized KFSBC and DFSBC are defined at the mean free surface. The flow properties of linear waves can be expressed as

$$\text{Wave elevation}: \quad \eta = \frac{H}{2}\cos[k(x-ct)], \tag{6}$$

$$\text{Velocity potential}: \quad \varphi = \frac{gH}{2\omega}\frac{\cosh[k(z+d)]}{\cosh(kd)}\sin[k(x-ct)], \tag{7}$$

$$\text{Dispersion relation}: \quad c^2 = \frac{\omega^2}{k^2} = \frac{g}{k}\tanh(kd), \tag{8}$$

$$\text{Horizontal flow velocity}: \quad u = \frac{\pi H}{T}\frac{\cosh[k(z+d)]}{\sinh(kd)}\cos[k(x-ct)], \tag{9}$$

$$\text{Vertical flow velocity}: \quad w = \frac{\pi H}{T}\frac{\sinh[k(z+d)]}{\sinh(kd)}\sin[k(x-ct)], \tag{10}$$

where x and z are the horizontal and vertical positions, k (=$2\pi/\lambda$) is the wave number, c (=λ/T) is the wave speed, and ω is the wave frequency. Depending on the water depth, the waves can be categorized as shallow water waves when $d/\lambda < 1/20$, as

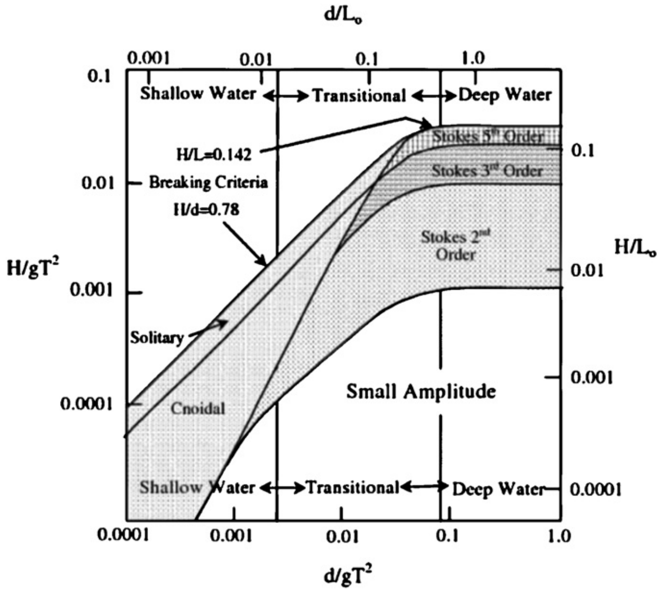

Fig. 8. The applicability of various wave theories [45,47].

intermediate-depth waves when $1/20 < d/\lambda < 1/2$, and as deep water waves when $d/\lambda > 1/2$.

When the wave amplitude is not small, the waves become nonlinear. The linearized KFSBC and DFSBC are not satisfied, and the nonlinear KFSBC and DFSBC can be written as

$$\begin{aligned}&\text{KFSBC}: \quad \frac{\partial \eta}{\partial t}+\frac{\partial \phi}{\partial x}\frac{\partial \eta}{\partial x}=-\frac{\partial \phi}{\partial z} \quad \text{at} \quad z=\eta(x,t),\\ &\text{DFSBC}: \quad \frac{P}{\rho}+\frac{1}{2}\left[\left(\frac{\partial \phi}{\partial x}\right)^2+\left(\frac{\partial \phi}{\partial z}\right)^2\right]-\frac{\partial \phi}{\partial t}+gz=C(t) \quad \text{at} \quad z=\eta(x,t),\end{aligned} \tag{11}$$

where $C(t)$ is constant.

The nonlinear solution can only be obtained by solving Eqs. (5)–(8). The nonlinear higher order solution is generally the superposition of additional components, which are at higher wave frequencies, on the fundamental linear wave-theory terms. There have been numerous nonlinear higher order wave theories developed since the 1800s. The Stokes theory [42,43] is the most well known and studied. An extension of the fifth-order Stokes waves was presented by Skjelbreia and Hendrickson [44], and it has been widely used in engineering applications. The wave profile and the velocity potential of the fifth-order Stokes waves are given as

$$\text{Wave elevation}: \quad k\eta=\sum_{n=1}^{5}A_n\cos[nk(x-ct)], \tag{12}$$

$$\text{Velocity potential}: \quad \frac{k\phi}{c}=\sum_{n=1}^{5}C_n\cosh[nk(z+d)]\sin[nk(x-ct)]. \tag{13}$$

The applicability of various wave theories was studied in Refs. [45,46], and the figure plotted by Le Méhauté is shown in Fig. 8. It illustrates the validity limitation of these approximation approaches for different wave conditions. A review of the introduction of wave theories and the applications to wave load prediction on offshore structures is provided by Sarpkaya [47], and a more comprehensive review of the theories and the applications of linear and nonlinear waves is given in Ref. [48].

In the real world, waves are not monochromatic. There are a large variety of waves with different frequencies, phases, and amplitudes. For an adequate description of the free surface, a large number of waves must be superimposed together. Usually, we use spectra to describe them. Furthermore, the behavior of waves is rather random. In this situation, the waves are called irregular waves. The random wave field can be approximated by using an infinite sum of sinusoidal components propagating with various wavelengths. Pierson–Moskowitz spectrum [49] and Jonswap spectrum [50] are the two most widely used spectra profiles. Refer to textbooks such as [48,51] for wave theory and [35,47,52] for wave–body interactions.

3. Analytical maximum power extraction studies

Analytical methods can be sorted, with or without detailed descriptions, by WEC systems. The first analytical study of a point absorber's power output focused on maximum efficiency, without the detailed description of the device, in 1975 [53,54]. The linearized equation of motion for the point absorber device in heave is

$$(m+m_r)\ddot{z}+R_r\dot{z}+Sz=F_{PTO}+F_{ext}, \tag{14}$$

where m is the mass of the body, m_r is the hydrodynamic coefficient of added mass, R_r is the radiation damping coefficient, S is stiffness of hydrostatic restoring force, F_{PTO} is the vertical force due to power-take-off mechanism, and F_{ext} is excitation force. The maximum energy absorption $P_{\max}$ for different incident wave frequencies can be reached when the oscillating body system is at resonance. Based on the linear deep-water wave assumptions, the time averaged optimal power absorption at resonance is

$$P_{\max}=\frac{1}{8R_r}|F_{ext}|^2. \tag{15}$$

An absorption width $L_{\max}$ is defined as

$$L_{\max}=\frac{P_{\max}}{J}=\frac{\lambda}{2\pi}, \tag{16}$$

$$J=\frac{\rho g^2TH^2}{32\pi}, \tag{17}$$

where J is the wave energy flux for linearized deep water waves. Note that Evans [55], Mei [56] and Newman [57] also independently derived the same result in Eq. (16) using similar approaches in 1976.

The maximum power that can be absorbed from waves and the absorption width is derived based on linear wave theory and consideration of wave radiation and diffraction. Budal and Falnes [58] proposed another upper limit (also referred to as Budal's upper bound) for wave power that is absorbed by a given submerged body volume V

$$\frac{P_u}{V}<\frac{\pi\rho gH}{4T}, \tag{18}$$

where the diffraction effect is neglected, and the size of the body is assumed to be small compared with the wave length. The two curves represent the theoretical prediction of the maximum wave energy that can be captured by a semi-submerged heaving body with optimum heaving amplitude. The power output for a practical device is below the two upper limits, and the maximum power that can be absorbed is about half of $P_{\max}$, when a phase control method is applied [29].

4. Modeling methods

The dynamic response of point absorbers can be calculated by solving Eq. (1), and power generation can be predicted using Eq. (3). Theoretically, the hydrodynamic forces that affect the point absorber motion can be obtained analytically,[1] empirically

[1] The analytical method can be derived by an equivalent linearization of the empirical calculation. Therefore, the former can be viewed as a special case of the latter.

or numerically, depending on the modeling purpose, the operational condition, and the detailed design. These modeling methods evolved from modeling ship hydrodynamics and offshore floating structures. Therefore, we apply the methods for naval architecture and offshore engineering when we review modeling methods for predicting the hydrodynamics of point absorber systems.

4.1. Analytical methods

A common approach to determine the hydrodynamic force analytically is to presume that the force is the sum of wave diffraction and wave radiation components,

$$\mathbf{F_{hd}} = \mathbf{F_R} + \mathbf{F_D}, \tag{19}$$

where the subscripts '**R**' and '**D**' represent the radiation and diffraction terms, respectively. The radiation components include an added-mass component and a radiation damping term.

$$\mathbf{F_R} = \mathbf{A}\ddot{\mathbf{X}} + \mathbf{B}\ddot{\mathbf{X}}, \tag{20}$$

where **A** and **B** are the hydrodynamic added-mass and damping coefficients. The wave excitation force, induced by wave diffraction, includes a diffraction component F_{DF}, due the present of the floating body, and a Froude–Krylov force component F_{FK}, generated by undisturbed incident waves.

$$\mathbf{F_D} = \int_{S_w} \frac{\partial \phi}{\partial t}\mathbf{n}\, ds = \int_{S_w} \frac{\partial(\phi_I + \phi_D)}{\partial t}\mathbf{n}\, ds = \mathbf{F_{FK}} + \mathbf{F_{DF}}, \tag{21}$$

where S_w is the immersed surface on the body, **n** is the unit normal vector, ϕ_I is the incident wave velocity potential and ϕ_D is the diffraction velocity potential.

The velocity potential are then solved analytically, and most of the analytical solutions were derived through the use of linear wave theory. Many analytical studies can be found in the literature. For examples, Newman [59] calculated the excitation force and moment though the use of Haskind relation. Yeung [60] proposed an analytical method for calculating the added mass and damping coefficients for offshore engineering applications. The paper suggests a method to calculate the coefficient using the Eigen functions. In addition, an analytical derivation of the hydrodynamic coefficients of a floating hemisphere undergoing forced periodic oscillations was presented in Ref. [61]. The analytical methods have also been widely used in ocean engineering problems, especially for an array of cylinders [62,63].

In reality, the viscous damping effect is important for modeling the hydrodynamics of point absorbers, and neglecting the viscous drag will result in an unrealistic large prediction on the response of the device and on power extraction performance, particularly near the resonance. Discussion on energy loss due to viscous damping can be found in [34,64]. A common approach to include the viscous drag effect in the modeling is to add a quadratic damping term to the non-viscous hydrodynamic forces. More details on the calculation of viscous damping force are discussed in Section 4.3.

In the past decade, many researchers have used the analytical method to calculate the power output of point absorbers [26,65–67]. In addition to a single unit, this method has been used to study arrays of WEC systems. For example, through the use of linear theory and multiple-scale approximation, Garnaud and Mei [68] presented an analytical solution to the wave energy extraction using infinite strips of buoys and a circular array. The study showed that an array of heaving wave-absorbing buoys could have a broader range of wave frequencies than a single large buoy, with good energy-absorbing efficiency. In general, analytical methods are very efficient for providing a quick performance estimation of point absorbers with simple geometries.

4.2. Boundary integral equation methods

Boundary integral equation method (BIEM), also referred to as boundary element method, is an advanced potential flow method that can be used for handling more complicated geometries. The governing equation, Eq. (4), is formulated in a boundary integral equation form, which is derived by introducing a Green's function $G(\mathbf{p},\mathbf{q})$, where **p** and **q** represent the field point and the source point, respectively. The boundary integral equation obtained through the use of Green's third identity gives

$$\alpha(\mathbf{p})\phi(\mathbf{p}) + \int_S \phi(\mathbf{p})G_n(\mathbf{p},\mathbf{q}) - \phi_n(\mathbf{p})G(\mathbf{p},\mathbf{q})\, ds = 0, \tag{22}$$

where S indicates the boundaries of the fluid domain, $\alpha(\mathbf{p})$ is the internal angle formed at the boundaries, $G_n = \nabla G\cdot\mathbf{n}$ and $\phi_n = \nabla\phi\cdot\mathbf{n}$, with **n** being the normal vector at **q**. The boundary surfaces are discretized into panels. By using Dirichlet- and Neumann-type boundary conditions, the potential flow field can be obtained by solving the resulting system of linear equations numerically.

After the potential flow field is obtained, the pressure on the body surface is evaluated using Bernoulli's equation,

$$p = -\rho\left(\phi_t + \frac{1}{2}\nabla\phi\cdot\nabla\phi + gz\right). \tag{23}$$

The forces **F** and moment **M** acting on the body are calculated by integrating the pressure on the immersed body surface,

$$\mathbf{F} = \int_{S_B} p\mathbf{n}\, ds; \qquad \mathbf{M} = \int_{S_B} p\mathbf{n}\times\mathbf{r}\, ds, \tag{24}$$

where **r** is the distance vector from the center of rotation. The viscous damping coefficient can be estimated based on the empirical solution, following the same approach used in the analytical method.

Regarding the simulation of the interaction between waves and floating bodies, two types of BIEM approaches have been used for modeling. One follows a weakly nonlinear theory that uses a perturbation expansion for the solution (the theory of wave radiation and diffraction) and specifies the boundary conditions at the mean free surface and body-surface through the use of Taylor series expansion. The other method uses a fully nonlinear time-domain approach.

The weakly nonlinear approach has the advantage of having the same coefficient matrix for the system of equations solved at every time step. One can solve the problem in the time domain [69] or in the frequency domain, which is the method used in the panel code WAMIT [70]. In the frequency domain calculation, radiation, diffraction, and excitation forces are calculated through the use of the linear superposition principle, which is limited to smaller amplitude waves (weak nonlinear waves) [71]. The complexity of the method increases significantly for higher order schemes. Examples of studies that used this weak nonlinear approach for wave radiation and diffraction problems can be found in Refs. [72–78]. A discussion on the use of linear and second-order approaches for predicting the wave excitation of floating bodies was given in Ref. [79].

The fully nonlinear time domain approach for wave analysis was first proposed by Longuet-Higgins and Cokelet, using a Mixed Eulerian–Lagrangian (MEL)-type method for modeling surface waves [80,81]. Fully nonlinear boundary conditions were applied on the instantaneous water free surface and body surface, and the free surface was computed using a tracking method. With BIEM, the computational domain is discretized along the domain boundaries, including the free surface and the body surface. Therefore, the coefficient matrix for the system of equations should be updated at every time step, and the method is only solved in

time domain. A high order Runge–Kutta scheme is often used to update the time varying free surface and body surface. The nonlinear time-domain approach is more accurate for modeling the highly nonlinear interaction between waves and floating bodies. Using this approach, researchers successfully predicted the nonlinear irregular wave radiation [82] and diffraction [83] of vertical cylinders, as well as the ventilating entry of a surface-piercing hydrofoil [84].

Additionally, modeling floating bodies in numerical wave tank requires a boundary that generates waves and absorbs reflected waves at the same time, and a boundary that absorbs outgoing waves. Over the years, many efforts have been made to develop a numerical method to simulate these types of boundaries, without creating additional numerical disturbances. A review on unbounded domains, with various types of artificial boundary conditions and absorbing methods, was given in [85]. Most of the studies between the 1970s and the 1990s were based on potential flow theory. In particular, a sponge-layer method was proposed by Israeli and Orszag [86], in which an artificial damping layer (zone) was implemented to attenuate the outgoing wave before it reached the outer boundary. Similar approaches also were proposed in Refs. [87,88].

The frequency domain BIEM is the most commonly used BIEM method for modeling the hydrodynamics and the power generation performance of point absorber systems. The method is used for calculating the non-viscous hydrodynamic forces described in the analytical method. McCabe et al. [89] demonstrated an example of modeling the responses of axisymmetric bodies in irregular waves using WAMIT. The method was combined with a Laplace transfer-function formulation to model the dynamics of the floating body in time domain. Given that the BIEM can be used for modeling more complex geometry, the method has been widely used in the studies of not only point absorber systems but also a wide variety of WEC systems. For examples, the method was used to study the power generation performance of floating pitching devices [9,90], a modified version of the Salter's Duck by Cruz and Salter [91], and a bottom-hinged surge-pitching plate [92]. Moreover, a recent study utilized the frequency domain BIEM to perform a series of studies on the power extraction performance of eight selected WEC systems, including five heaving absorber systems with different design principles [64]. The study also analyzed the annual power generation performance and the capture efficiency at five different site locations. Moreover, several researchers have used the method in the study of control and tuning strategies for heaving absorbers [93–96]. For the analysis of array systems for point absorbers, the interaction effect could be considered through the use of a multiple-scattering method [67,97,98]. In particular, Vicente et al. [98] used the method to analyze the dynamics of the array system with inter-body connections and bottom slack-mooring lines.

4.3. Viscous drag calculation for potential flow solution

Generally, the additional viscous damping term follows the drag term in the Morison's equation. The Morison's equation was proposed by four authors, J.R. Morison, M.P. O'Brien, J.W. Johnson and S.A. Schaaf, at the University of California, in 1950 [99], and the drag term was given as

$$F_d = -\frac{1}{2}\rho C_d A_c (u - u_b)|u - u_b| \tag{25}$$

where C_d is the quadratic drag (viscous damping) coefficient, ρ indicates the density of sea water, A_c is the characteristic areas, u is the flow velocity, and u_b is the velocity of the body. Generally, the value of viscous damping coefficient depends on the body geometry, the Reynolds number and the Keulegan–Carpenter number. More details of the use of quadratic drag approach and the appropriate values for the empirical coefficient can be found in [47,100].

In addition, the empirical viscous damping coefficient data are limited to existing simple geometry. For practical point absorber geometry, the hydrodynamic forces may have to be evaluated by conducting additional wave tank tests [101] or prescribed motion CFD simulations [102,103] if existing data is not available.

4.4. Navier–Stokes equation methods

The viscous effects of boundary layer separation, turbulence, wave breaking, and overtopping are important to the prediction of hydrodynamic forces of the devices. The potential flow method cannot capture them. Therefore, modelers often turn to a fully viscous solution by implementing the Navier–Stokes equation methods (NSEM). The velocity vector $\mathbf{U}$ and pressure p of the incompressible flow field are obtained by solving the continuity equation and the momentum equations, which are given as

$$\begin{aligned} &\nabla \cdot \mathbf{U} = 0, \\ &\rho(\mathbf{U}_t + \mathbf{U} \cdot \nabla \mathbf{U}) = -\nabla p + \mathbf{F}_b + \nabla \cdot \mathbf{T}, \end{aligned} \tag{26}$$

where $\mathbf{U}_t$ is the time derivative of $\mathbf{U}$, $\mathbf{F}_b$ is the body force vector (such as gravity), and $\mathbf{T}$ indicates the stress tensor. The computational domain can be discretized using a finite difference/volume/element method, and the resulting system of linear equations can be solved directly, or preferably, through iterations using an appropriate linear equation system solver. A well known Semi-Implicit Method for Pressure-Linked Equations (SIMPLE) algorithm [104] and its variants have been widely used for solving Navier–Stokes equations. More details on the numerical discretization methods, as well as the physical phenomena, are given in Refs. [105,106]. The force and moment calculation is similar to that applied in the potential flow theory, except that the frictional force also is included in the calculation.

Basically, using the Navier–Stokes equation-based method for modeling the hydrodynamics of floating bodies in waves involves the calculation of the free surface in a numerical wave tank and the simulation of the turbulent flow. In general, two types of approaches have been applied for predicting the free surface. One is the surface tracking method, which treats the free surface as a sharp boundary and updates it with time [107]. However, the method does not have the ability to model wave breaking and overtopping. The other is the interface-capturing method, where the simulation is performed on a grid that includes both air and water phases. Marker-and-Cell (MAC) method [108], Volume Of Fluid (VOF) method [109], and the level set approach [110,111] are the most often used interface-capturing methods. In particular, the VOF method is the most widely used for commercial and open source computational fluid dynamics (CFD) codes. Review of these methods and their application to wave hydrodynamics can be found in [106,112]. The artificial damping layer method also is widely used in the Navier–Stokes equation-based approaches for absorbing the outgoing and reflecting waves in the wave–body interaction simulation. For example, Lara et al. [113] combined the sponge-layer method, with an internal-wave maker method [114], to model the wave generating-absorbing boundary and simulated the interaction between waves and permeable structures.

In general, four types of numerical methods are applied for turbulent flow modeling, including direct numerical simulations (DNS) [115], large eddy simulations (LES) [116,117], Reynolds-averaged Navier–Stokes (RANS) methods, and detached eddy simulations (DES). The corresponding computational cost for DNS and LES is very high DNS, and the two models are often viewed as a research tool in the study of turbulence, particularly for most floating body dynamics problems. Therefore, the RANS

method is the most widely used scheme for modeling turbulent flow. The unsteadiness of the turbulence is time averaged and the computation of turbulent flow relies on simplified engineering approximations. DES is a hybrid method that combines the RANS and LES methods. It handles the near wall region, with a RANS-type model, and treats the rest of the flow field using a LES-type method. Different types of RANS models are designed for different turbulent flows. The physical phenomena and the basic assumptions for each turbulence model were comprehensively reviewed by Wilcox [118].

Using NSEM for modeling floating body dynamics often involves the handling of moving boundary and mesh deformation. Several methods have been developed over the years, including: (1) boundary-fitted mesh morphing method, which is the most common approach and typically involves the use of Arbitrary Lagrangian–Eulerian methods [119]; (2) overset method (also referred to as Chimera approach), which use a multi-mesh system that solve the problem using separately generated but overlapping meshes through iterations [120]; (3) immersed boundary method, which introduces a body force term in the governing equation to represent the boundary surface [121]; (4) Smooth Particle Hydrodynamics (SPH) method [122], which is a mesh free Lagrangian method and uses a smoothing kernel to approximate a delta function, with many sampling points in the fluid domain. Generally, boundary-fitted mesh morphing method and the overset method are the most widely used models for solving wave and floating body dynamics problems.

NSEM has often been used for studying the complex nonlinear wave and floating body interaction in ocean engineering problems. For example, Moctar et al. [123] used a RANS model to analyze the wave load of a jack-up platform under freak waves, where the VOF method was adopted for the free-surface calculation and was coupled with a finite element model for the structure's stress analysis. The study demonstrated the significance of using a Navier–Stokes type approach, where the effects of wave run-up on the platform leg and the impact-related wave loads on the hull were all considered. Their study also showed that the difference between the shear and overturning moment for the platform under freak waves calculated from the Morison's approach, and those obtained from the RANS calculation, can increase up to 25%, especially for larger and breaking waves.

A few studies on the fluid–structure interaction of WEC systems were performed using the Navier–Stokes-type approaches. A RANS code (COMET) was applied by Agamloh et al. [124] to model the dynamics of a single buoy and a double buoy system in waves. The PTO mechanism was considered as the damping system based on the energy that was captured. Studies on the Wave-driven, Resonant, Arcuate-action, Surging Point-Absorber (WRASPA) were presented by Bhinder et al. [125,126]. The authors performed a series of studies using a RANS model to investigate the hydrodynamics of a floating-point absorber [127]. The power take off was represented using a mass–spring–damper system, and the maximum power that this particular device generated, with a constant value spring–damper system, was examined.

5. Discussion

In Section 4, we have summarized the existing numerical methods for modeling the dynamic response of point absorber in waves and for predicting the power generation of the system. Here, we provide further discussion and insights on these methods.

Table 1 illustrates the features of each method for modeling point absorber systems. Depending on the purpose of the study, each method has its advantages and limitations. The analytical solution only can be used for simple geometries, while BIEM and NSEM can be used for more complicated and realistic ones. The analytical method and the frequency domain BIEM model the system dynamics in a sequential approach and use the treatments of radiation and diffraction problems for estimating the hydrodynamic forces. Therefore, the utilization of these two methods is generally limited to relatively smaller waves. On the contrary, the time domain BIEM and NSEM fully couples the flow field simulation with the solution for the equation of motion at each time step. The time domain BIEM is feasible for capturing the fully nonlinear interaction between waves and the floating body, except for wave breaking, overtopping and viscous flow separation. A floating body dynamics CFD (NSEM) simulation is needed to fully capture all the nonlinear interaction between waves and the device, including viscous flow separation, turbulence, wave breaking and overtopping.

An example for modeling the power generation performance of a two-body floating-point absorber system is presented to demonstrate the utilization of these methods. The two most commonly used methods, a frequency-domain BIEM and a NSEM (CFD), were selected. In the frequency domain BIEM, the hydrodynamic forces were calculated using WAMIT, and the viscous damping coefficient was estimated based on the empirical solution of [47,100]. The details of the device geometry and the numerical settings in the CFD simulation were described in Ref. [127]. To compare the results obtained from the two methods, the computational time for each model is shown in Table 2, and the power generation performance is plotted against incident wave periods in Fig. 9. It is found that the frequency-domain BIEM is much more cost-effective. However, the selection of viscous damping coefficients has a significant influence on the frequency-domain BIEM results, particularly near resonance. Note that the maximum power generally occurs when point absorber systems are close to resonance. The calculation of viscous damping is important to predict the power and may lead to significant uncertainty in the prediction results. For example, Babarit et al. [64] showed that if the drag coefficients were varied by a factor of 4, the effect on power generation could be up to 30%.

Table 1
Features of hydrodynamic modeling methods.

Methods	Features				
	Viscous effects	Dynamic coupling complexity	Wave/body interaction	Accuracy	
				Hydrodynamics modeling	System dynamics modeling
Analytical	Empirical	Radiation and diffraction theory	Linear	Affected by the prediction of viscous damping	Limited to waves with relatively smaller amplitude
Frequency domain BIEM	Empirical	Radiation and diffraction theory	Non-breaking waves	Affected by the prediction of viscous damping	
Time domain BIEM	Empirical	Fully coupled time domain simulation	Non-breaking waves	Affected by the prediction of viscous damping	Very good Fully nonlinear
NSEM: floating-body dynamics CFD	Solves Navier–Stokes equation	Fully coupled time domain simulation	Fully nonlinear and breaking waves	Very good	

Table 2
Run-time benchmark for modeling point absorber WEC systems.

Hydrodynamics modeling	Discretization	Number of panels/meshes	Wall clock time
Frequency domain BIEM (WAMIT) & quadratic drag	Boundary discretization	5096 (low-order panels)	2804 s[a] (30 wave frequencies)
NSEM: floating body-dynamics CFD	Computational domain discretization	≈1 million (finite volume mesh)	12 h on 64 cores[b] (one wave frequency)

[a] On a 3.33 GHz Intel i5 processor with 8 GB of memory.
[b] Each compute node consists of dual socket/quad-core 2.93 GHz Intel Nehalem processor, with 12 GB of memory shared by all 8 cores.

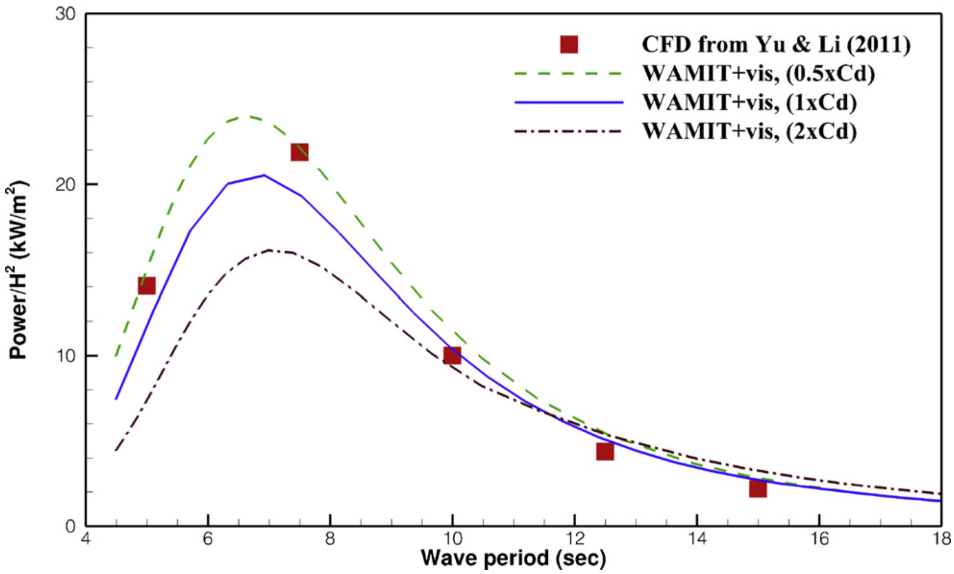

Fig. 9. Power generation prediction from NSEM and BIEM (C_{PTO} = 507 kN s m^{-1}).

For operational wave conditions, where waves are relatively small and linear theory are generally applicable, and the non-viscous hydrodynamic forces are dominated by radiation and diffraction components. The frequency domain BIEM is the most commonly used method for modeling the power generation performance of point absorber systems. However, the viscous damping coefficients need to be carefully selected. The drag coefficient depends on the device geometry, the scale and the relative velocity between the body and the flow around it. The drag coefficient becomes much larger when the Reynolds number and the Keulegan–Carpenter number are smaller [100]. In addition, after the frequency domain hydrodynamic forces are obtained, the response of point absorbers can be calculated using a frequency domain approach or a time domain approach. The frequency domain solution represents the steady-state response due to the sinusoidal excitation of regular waves. The time domain approach solves the Cummins equations [128] and are often used for modeling the dynamics of the system in irregular waves, particularly for the study of optimal control strategies. The methods and the relationship between the parameters in the frequency domain approach and those in the time domain approach were well summarized by Ogilvie [129].

For survivable conditions, a time-domain fully nonlinear BIEM model or NSEM is more applicable. In reality, point absorbers are designed to sustain the extreme wave load during storms. The device may subject to waves with a typical 100-year significant wave height in the range between 8 m and 13 m. Under these waves, breaking and overtopping waves often occur and the effect of the nonlinear interaction between waves and the floating body on the dynamic response of the system is significant. Only NSEM models have the capability of modeling all the complex nonlinear hydrodynamics. However, longer computational time is required. The actual computational time generally depends on many factors, including processor speed, convergence criterion, mesh quality, parallel efficiency, and the complexity of the interaction between waves and the floating body. Thus, one may have to compromise accuracy against computational cost.

6. Conclusion

Four numerical methods for modeling the point absorber systems have been reviewed in this paper; each method has its own strength and limitation. For idea analysis, analytical method is sufficient and effective. For modeling a practical point absorber WEC system, frequency domain BIEM and NSEM are the most commonly used method depending on the wave condition. In operational condition, the frequency domain BIEM, with a carefully selected viscous damping, is generally used for power generation performance analysis, design and optimization. They tends to be easier to combine with the modeling techniques for other aspects of the point absorbers such as the power system. On the other hand, NSEM is typically used for detailed analysis or for survivability analysis, where the nonlinear interaction between waves and the WEC system is significant. Time domain fully nonlinear BIEM is more appropriate in the transition between these those conditions and for developing active control strategies.

In additional to the point absorbers, there are a wide variety of WEC systems such as bottom hinged device and oscillating water column. Similar modeling philosophy can be applied to them. However, the dominant physical phenomenon for each system varies. For examples, additional nonlinear effects on the hydrodynamics of the system due to wave breaking and overtopping, can be significant for a bottom-hinged pitching plate. The additional constraint due to mooring connections can be essential for a floating device oscillating water column. The prediction of these additional forces and the level of complexity of the interaction between forces and

system dynamics will affect the accuracy of the modeling method, particularly the frequency domain BIEM, and the overall computational time. We will investigate these features in future.

Acknowledgement

We would like to acknowledge the U.S. Department of Energy's Wind and Water Power Program for funding this work under the funding agreement of 20067.

References

[1] Ross D. Power from sea waves. 1st ed. United Kingdom: Oxford University Press; 1995.
[2] Salter S. Wave power. Nature 1974:720–4.
[3] Ocean Power Technologies; 2011, May [Online]. http://www.oceanpowertechnologies.com.
[4] Wavebob; 2011, May [Online]. http://www.wavebob.com/home/.
[5] Wavestar [Online]. http://wavestarenergy.com/.
[6] Wave Dragon [Online]. http://www.wavedragon.net/.
[7] IEA-OES. International Energy Agency Ocean Energy System; 2011, May [Online] http://www.iea-oceans.org/index.asp.
[8] IEC. International Electrotechnical Commission Marine Energy Technical Committee; 2011, May [Online] http://www.bsigroup.com/en/Standards-and-Publications/Committee-Members/Committee-member-news/Summer-2007/New-Committee-IECTC-114-Marine-Energy/.
[9] McCabe A, Bradshaw A, Meadowcroft J, Aggidis G. Developments in the design of the PS Frog Mk 5 wave energy converter. Renewable Energy 2006;31(2):141–51.
[10] Kraemmer D, Ohl C, McCormick M. Comparison of experimental and theoretical results of the motions of a McCabe Wave Pump. In: Proceedings of the fourth European wave power conference, vol. 1. 2000.
[11] Pelamis Wave Power [Online]. http://www.pelamiswave.com/.
[12] Salter S. The swinging mace. In: Proceedings of the workshop on wave energy R&D. 1992. p. 197–206.
[13] Whittaker T, Collier D, Folley M, Osterried M, Henry A, Crowley M. The development of Oyster—a shallow water surging wave energy converter. In: Proceedings of the 7th European wave and tidal energy conference. 2007. p. 11–4.
[14] Aquamarine Power Oyster [Online]. http://www.aquamarinepower.com/technology.
[15] Heath T, Whittaker T, Boake C. The design, construction and operation of the LIMPET wave energy converter. In: Proceedings of the 4th European wave energy conference. 2000. p. 49–55.
[16] Ohneda H, Igarashi S, Shinbo O, Sekihara S, Suzuki K, Kubota H, et al. Construction procedure of a wave power extracting caisson breakwater. In: Proceedings of the 3rd symposium on ocean energy utilization. 1991. p. 171–9.
[17] Clément A, McCullen P, Falcão A, Fiorentino A, Gardner F, Hammarlund K, et al. Wave energy in Europe: current status and perspectives. Renewable and Sustainable Energy Reviews 2002;6(5):405–31.
[18] Kofoed J, Frigaard P, Friis-Madsen E, Sørensen H. Prototype testing of the wave energy converter wave dragon. Renewable Energy 2006;31(2):181–9.
[19] Vicinanza D, Frigaard P. Wave pressure acting on a seawave slot-cone generator. Coastal Engineering 2008;55(6):553–68.
[20] Lilypad [Online]. http://www.energyisland.com/projects/lilypad/lilypad.html.
[21] Weber J, Mouwen F, Parish A, Robertson D. Wavebob—research & development network and tools in the context of systems engineering. In: Proceedings of the eighth European wave and tidal energy conference. 2009.
[22] Salter S, Lin C-P. The sloped IPS wave energy converter. In: Proceedings of the 2nd European wave energy conference. 1995. p. 337–44.
[23] Payne GS, Taylor JRM, Bruce T, Parkin P. Assessment of boundary-element method for modelling a free-floating sloped wave energy device. Part 1. Numerical modelling. Ocean Engineering 2008;35(3–4):333–41.
[24] Payne GS, Taylor JRM, Bruce T, Parkin P. Assessment of boundary-element method for modelling a free-floating sloped wave energy device. Part 2. Experimental validation. Ocean Engineering 2008;35(3–4):342–57.
[25] Evans D. Power from water waves. Annual Review of Fluid Mechanics 1981;13(1):157–87.
[26] Falcão AFdO. Wave energy utilization: a review of the technologies. Renewable and Sustainable Energy Reviews 2010;14(3):899–918.
[27] Sarmento AJNA, Neumann F, Brito-Meto A. Non-technical barriers to large-scale wave energy utilisation. In: Proceedings of the 2004 new and renewable energy technologies for sustainable development. 2004. p. 225–33.
[28] Energy USDo. DOE; 2010, December [Online] http://www1.eere.energy.gov/windandhydro/hydrokinetic/listings.aspx?type=Tech.
[29] Falnes J. A review of wave-energy extraction. Marine Structures 2007;20(4):185–201.
[30] Khan J, Bhuyan G, Moshref A. An assessment of variable characteristics of the Pacific Northwest region's wave and tidal current power resources, and their interaction with electricity demand & implications for large scale development scenarios. Surrey: PowerTech Lab; 2008 [Internal Report].
[31] Brooke J. Wave energy conversion. Elsevier Science; 2003.
[32] Cruz J. Ocean wave energy. 1st ed. Berlin, Germany: Springer; 2008.
[33] McCormick M. Ocean wave energy conversion. 2nd ed. Dover; 2007.
[34] Falnes J. Ocean waves and oscillating systems; 2002.
[35] Faltinsen O. Wave loads on offshore structures. Review of Fluid Mechanics 1990;22(1):35–56.
[36] Evans D. Maximum wave-power absorption under motion constraints. Applied Ocean Research 1981;3(4):200–3.
[37] Pizer DJ. Maximum wave-power absorption of point absorbers under motion constraints. Applied Ocean Research 1993;15:227–34.
[38] Muliawan M, Gao Z, Moan T, Babarit A. Analysis of a two-body floating wave energy converter with particular focus on the effect of mooring system on energy capture. In: Proceedings of the 30th international conference on ocean, offshore, and artic engineering. 2011.
[39] Drew B, Plummer A, Sahinkaya M. A review of wave energy converter technology. Proceedings of the Institution of Mechanical Engineers Part A: Journal of Power and Energy 2009;223(8):887–902.
[40] Airy G. Tides and waves. Encyclopedia Metropolitana 1841;5: 24l–396l.
[41] Clarke JA, Connor G, Grant AD, Johnstone CM. Design and testing of a contra-rotating tidal current turbine. Proceedings of the Institution of Mechanical Engineers Part A: Journal of Power and Energy 2007;221(A2):171–9.
[42] Stokes G. On the theory of oscillating waves. Transactions of the Cambridge Philosophical Society 1847;8:441.
[43] Stokes G. On the effect internal friction of fluids on the motion of pendulums. Mathematics and Physics Papers 1880;3:1–10.
[44] Skjelbreia L, Hendrickson J. Fifth order gravity wave theory. In: Proceedings of the 7th conf. coastal eng. 1961. p. 184–96.
[45] Le Méhauté B. An introduction to hydrodynamics and water waves. New York: Springer-Verlag; 1976.
[46] Dean R. Relative validities of water wave theories. Journal of the Waterways, Harbors and Coastal Engineering Division 1970;96(1):105–19.
[47] Sarpkaya T. Wave forces on offshore structures. Cambridge; 2010.
[48] Mei CC, Stiassnie M, Yue DK-P. Theory and applications of ocean surface waves: nonlinear aspects. World Scientific; 2005.
[49] Pierson Jr W, Moskowitz L. A proposed spectral form for fully developed wind seas based on the similarity theory of SA Kitaigorodskii. Journal of Geophysical Research 1964;69(24):5181–90.
[50] Hasselmann K, Barnett T, Bouws E, Carlson H, Cartwright D, Enke K, et al. Measurements of wind-wave growth and swell decay during the Joint North Sea Wave Project (JONSWAP). Ergnzungsheft zur Deutschen Hydrographischen Zeitschrift Reihe 1973;8(12).
[51] Tucker MJ, Pitt EG. Waves in ocean engineering. 1st ed. Elsevier; 2001.
[52] Newman JN. Marine hydrodynamics. 1st ed. Cambridge, MA, USA: The MIT Press; 1977.
[53] Budal K, Falnes J. A resonant point absorber of ocean-wave power. Nature 1975;256:478–9 [corrigendum 257:626].
[54] Budal K, Falnes J. Power generation from ocean waves using a resonant oscillating system. Marine Science Communication 1975;1:269–88.
[55] Evans D. A theory for wave-power absorption by oscillating bodies. Journal of Fluid Mechanics 1976;77(01):1–25.
[56] Mei CC. Power extraction from water waves. Journal of Ship Research 1976;20:63–6.
[57] Newman J. The interaction of stationary vessels with regular waves. In: Proceedings of the 11th symposium on naval hydrodynamics. 1976. p. 491–501.
[58] Budal K, Falnes J. Interacting point absorbers with controlled motion. Power from Sea Waves 1980:381–99.
[59] Newman J. The exciting forces on fixed bodies in waves. Journal of Ship Research 1962;6(3):10–7.
[60] Yeung RW. Added mass and damping of a vertical cylinder in finite-depth waters. Applied Ocean Research 1980;3(April (3)):119–33.
[61] Hulme A. The wave forces acting on a floating hemisphere undergoing forced periodic oscillations. Journal of Fluid Mechanics 1982;121:443–63.
[62] Mclver P. Wave forces on arrays of floating bodies. Journal of Engineering Mathematics 1984;18(4):273–85.
[63] Siddorn P, Eatock Taylor R. Diffraction and independent radiation by an array of floating cylinders. Ocean Engineering 2008;(13):1289–303.
[64] Babarit A, Hals J, Muliawan MJ, Kurniawan A, Moan T, Krokstad J. Numerical benchmarking study of a selection of wave energy converters. Renewable Energy 2012;41:44–63.
[65] Erksson M, Isberg J, Leijon M. Hydrodynamic modelling of a direct drive wave energy converter. International Journal of Engineering Science 2005;43(17–18):1377–87.
[66] Berggren L, Johansson M. Hydrodynamic coefficients of a wave energy device consisting of a buoy and a submerged plate. Applied Ocean Research 1992;14(1):51–8.
[67] Mavrakos SA, Kalofonos A. Power absorption by arrays of interacting vertical axisymmetric wave-energy devices. Journal of Offshore Mechanics and Arctic Engineering 1997;119(4):224–31.
[68] Garnaud X, Mei C. Wave-power extraction by a compact array of buoys. Journal of Fluid Mechanics 2009;635:389–413.
[69] Kim Y, Kring D, Sclavounos P. Linear and nonlinear interactions of surface waves with bodies by a three-dimensional Rankine panel method. Applied Ocean Research 1997;19(5–6):235–49.
[70] Lee C. WAMIT theory manual. Cambridge, MA: Department of Ocean Engineering, Massachusetts Institute of Technology; 1995.

[71] Denis M. Some cautions on the employment of the spectral technique to describe the waves of the sea and the response thereto of oceanic systems. In: Proceedings of the offshore technology conference. 1973.
[72] Chen X, Ding Y, Zhang J, Liagre P, Niedzwecki J, Teigen P. Coupled dynamic analysis of a mini TLP: comparison with measurements. Ocean Engineering 2006;33(1):93–117.
[73] Kim M, Yue D. The complete second-order diffraction solution for an axisymmetric body. Part 2. Bichromatic incident waves and body motions. Journal of Fluid Mechanics 1990;211:557–93.
[74] Newman J. Second-harmonic wave diffraction at large depths. Journal of Fluid Mechanics 1990;213:59–70.
[75] Newman J. The second-order wave force on a vertical cylinder. Journal of Fluid Mechanics 1996;320:417–43.
[76] Wu G, Taylor R. The second order diffraction force on a horizontal cylinder in finite water depth. Applied Ocean Research 1990;12(3):106–11.
[77] Ran Z, Kim M. Nonlinear coupled responses of a tethered spar platform in waves. International Journal of Offshore and Polar Engineering 1997;7:111–8.
[78] Kim M. Second-order sum-frequency wave loads on large-volume structures. Applied Ocean Research 1991;13(6):287–96.
[79] Lee C, Newman J. Computation of wave effects using the panel method. Numerical models in fluid–structure interaction. Southampton, UK: WIT Press; 2004 [Preprint].
[80] Longuet-Higgins M, Cokelet E. The deformation of steep surface waves on water. I. A numerical method of computation. Proceedings of the Royal Society of London 1976;A350:1–26.
[81] Longuet-Higgins M, Cokelet E. The deformation of steep surface waves on water. II. Growth of normal-mode instabilities. Proceedings of the Royal Society of London A Mathematical and Physical Sciences 1978;364(1716):1.
[82] Bai W, Taylor RE. Higher-order boundary element simulation of fully nonlinear wave radiation by oscillating vertical cylinders. Applied Ocean Research 2006;28(4):247–65.
[83] Ferrant P, Touzé DL, Pelletier K. Non-linear time-domain models for irregular wave diffraction about offshore structures. International Journal for Numerical Methods in Fluids 2003;43(10–11):1257–77.
[84] Vinayan V, Kinnas S. A numerical nonlinear analysis of two-dimensional ventilating entry of surface-piercing hydrofoils with effects of gravity. Journal of Fluid Mechanics 2010;658:383–408.
[85] Tsynkov S. Numerical solution of problems on unbounded domains. A review. Applied Numerical Mathematics 1998;27(4):465–532.
[86] Israeli M, Orszag S. Approximation of radiation boundary conditions. Journal of Computational Physics 1981;41(1):115–35.
[87] Grilli S, Horrillo J. Numerical generation and absorption of fully nonlinear periodic waves. Journal of Engineering Mechanics 1997;123(10):1060–9.
[88] Romate J. Absorbing boundary conditions for free surface waves. Journal of Computational Physics 1992;99(1):135–45.
[89] McCabe A, Stallard T, Baker N, Yavuz H. Estimation of the responses of axisymmetric bodies in spread irregular waves. Ocean Engineering 2007;34(10):1371–82.
[90] McCabe A, Aggidis G, Stallard T. A time-varying parameter model of a body oscillating in pitch. Applied Ocean Research 2006;28(6):359–70.
[91] Cruz J, Salter S. Numerical and experimental modelling of a modified version of the Edinburgh Duck wave energy device. Proceedings of the Institution of Mechanical Engineers Part M: Journal of Engineering for the Maritime Environment 2006;220(3):129–47.
[92] Folley M, Whittaker TJT, Henry A. The effect of water depth on the performance of a small surging wave energy converter. Ocean Engineering 2007;34:1265–74.
[93] Yavuz H, Stallard T, McCabe A, Aggidis G. Time series analysis-based adaptive tuning techniques for a heaving wave energy converter in irregular seas. Proceedings of the Institution of Mechanical Engineers Part A: Journal of Power and Energy 2007;221(1):77–90.
[94] Falnes J. Optimum control of oscillation of wave energy converters. In: Proceedings of the eleventh international offshore and polar engineering conference. 2001. p. 567–74.
[95] Babarit ACH. Optimal latching control of a wave energy device in regular and irregular waves. Applied Ocean Research 2006;28(April (2)):77–91.
[96] Falcão AFdO. Modelling and control of oscillating-body wave energy converters with hydraulic power take-off and gas accumulator. Ocean Engineering 2007;34(October (14–15)):2021–32.
[97] Ricci P, Saulnier J, Falcão AFdO. Point-absorber arrays: a configuration study off the Portuguese West-Coast. In: Proceedings of the 7th European wave and tidal energy conference. 2007.
[98] Vicente P, Falcão A, Gato L, Justino P. Dynamics of arrays of floating point-absorber wave energy converters with inter-body and bottom slack-mooring connections. Applied Ocean Research 2009;31(4):267–81.
[99] Morison J, O'brien M, Johnson J, Schaaf S. The force exerted by surface waves on piles. Petroleum Transactions, AIME 1950;189:149–54.
[100] Sarpkaya TOJL. Oscillating flow about two and three-dimensional bilge keels. Journal of Offshore Mechanics and Arctic Engineering 1996;118:1–6.
[101] Yeung RW, Liao S-W, Roddier D. On roll hydrodynamics of rectangular cylinders. In: Proceedings of the international offshore and polar engineering conference. 1998. p. 445–53.
[102] Wilson RV, Carrica PM, Stern F. Unsteady RANS method for ship motions with application to roll for a surface combatant. Computers & Fluids 2006;35(5):501–24.
[103] Yu Y-H, Kinnas SA. Roll response of various hull sectional shapes using a Navier–Stokes solver. International Journal of Offshore and Polar Engineering 2009;19:46–51.
[104] Patankar SV, Spalding DB. A calculation procedure for heat, mass, and momentum transfer in three-dimensional flows. International Journal of Heat Mass Transfer 1972;15:1787.
[105] Patankar SV. Numerical heat transfer and fluid flow. Washington, DC: Hemisphere Publishing Corp.; 1980, 210 pp.
[106] Ferziger JH, Peric M. Computational methods for fluid dynamics. Springer; 2002.
[107] Gentaz L, Alessandrini B, Delhommeau G. 2D nonlinear diffraction around free surface piercing body in a viscous numerical wave tank. In: Proceedings of the 9th int. offshore and polar eng. conf., vol. 3. 1999. p. 420–6.
[108] Harlow F, Welch J. Numerical calculation of time-dependent viscous incompressible flow of fluid with free surface. Physics of Fluids 1965;8(12):2182.
[109] Hirt C, Nichols B. Volume of fluid (VOF) method for the dynamics of free boundaries. Journal of Computational Physics 1981;39(1):201–25.
[110] Sussman M, Smereka P, Osher S. A level set approach for computing solutions to incompressible two-phase flow. Journal of Computational Physics 1994;114(1):146–59.
[111] Sethian J, Smereka P. Level set methods for fluid interfaces; 2003.
[112] Lin P, Liu PL-F. Free surface tracking methods and their applications to wave hydrodynamics. Advances in Coastal and Ocean Engineering 1999;5:213–40.
[113] Lara J, Garcia N, Losada I. RANS modelling applied to random wave interaction with submerged permeable structures. Coastal Engineering 2006;53(5–6):395–417.
[114] Lin P, Liu PL-F. Internal wave-maker for Navier–Stokes equations models. Journal of Waterway, Port, Coastal, and Ocean Engineering 1999;125:207.
[115] Moin P, Mahesh K. Direct numerical simulation: a tool in turbulence research. Annual Review of Fluid Mechanics 1998;30(1):539–78.
[116] Lesieur M, Métais O. New trends in large-eddy simulations of turbulence. Annual Review of Fluid Mechanics 1996;28:45–82.
[117] Sirnivas S, Wornom S, Dervieux A, Koobus B, Allain O. A study of LES models for the simulation of a turbulent flow around a truss spar geometry. In: 25th International Conference on Offshore Mechanics and Arctic Engineering, OMAE, vol. 2006. 2006. p. 755–61.
[118] Wilcox D. Turbulence modeling for CFD. DCW Industries; 2006.
[119] Farhat C, Geuzaine P, Grandmont C. The discrete geometric conservation law and the nonlinear stability of ALE schemes for the solution of flow problems on moving grids. Journal of Computational Physics 2001;174(2):669–94.
[120] Chan WM. Overset grid technology development at NASA Ames Research Center. Computers & Fluids 2009;38(3):496–503.
[121] Peskin CS. The immersed boundary method. Acta Numerica 2002;11:479–517.
[122] Monaghan JJ. An introduction to SPH. Computer Physics Communication 1988;48:88–96.
[123] Moctar O, Schellin T, Jahnke T, Peric M. Wave load and structural analysis for a jack-up platform in freak waves. Journal of Offshore Mechanics and Arctic Engineering 2009;131:021602.
[124] Agamloh E, Wallace A, Jouanne AV. Application of fluid–structure interaction simulation of an ocean wave energy extraction device. Renewable Energy 2008;33(4):748–57.
[125] Bhinder M, Mingham C, Causon D, Rahmati M, Aggidis G, Chaplin R. A joint numerical and experimental study of a surging point absorbing wave energy converter (WRASPA). In: Proceedings of 28th int. conf. on ocean, offshore and arctic eng. 2009.
[126] Bhinder M, Mingham C, Causon D, Rahmati M, Aggidis G, Chaplin R. Numerical and experimental study of a surging point absorber wave energy converter. In: Proceedings of the 8th European wave and tidal energy conference. 2009.
[127] Yu Y-H, Li Y. A RANS simulation for the heave response of a two-body floating point wave absorber. In: Proceedings of the 21st international offshore (ocean) and polar engineering conference. 2011.
[128] Cummins, W. The impulse response function and ship motion. Technical Report 1661, David Taylor Model Basin-DTNSRDC, 1962.
[129] Ogilvie T. Recent progress towards the understanding and prediction of ship motions. In: 5th Symposium on Naval Hydrodynamics. 1964. p. 3–80.